The interaction between temperature and precipitation on the potential distribution range of *Betula ermanii* in the alpine treeline ecotone on the Changbai Mountain

Yu Cong [a], Yongfeng Gu [a,b], Wen J. Wang [a], Lei Wang [a], Zhenshan Xue [a], Yingyi Chen [a], Yinghua Jin [b,*], Jiawei Xu [a], Mai-He Li [d,e,b], Hong S. He [c], Ming Jiang [a]

[a] *Northeast Institute of Geography and Agroecology, Chinese Academy of Sciences, Changchun 130102, China*
[b] *Key Laboratory of Geographical Processes and Ecological Security in Changbai Mountains, Ministry of Education, School of Geographical Sciences, Northeast Normal University, Changchun 130024, China*
[c] *School of Natural Resources, University of Missouri, Columbia, MO 65211, USA*
[d] *Swiss Federal Institute for Forest, Snow and Landscape Research WSL, CH-8903 Birmensdorf, Switzerland*
[e] *School of Life Science, Hebei University, Baoding 071000, China*

ARTICLE INFO

ABSTRACT

Alpine treeline ecotones are highly sensitive to climate warming. The low temperature-determined alpine treeline is expected to shift upwards in response to global warming. However, little is known about how temperature interacts with other important factors to influence the distribution range of tree species within and beyond the alpine treeline ecotone. Hence, we used a GF-2 satellite image, along with bioclimatic and topographic variables, to develop an ensemble suitable habitat model based on the species distribution modeling algorithms in Biomod2. We investigated the distribution of suitable habitats for *B. ermanii* under three climate change scenarios (i.e., low (SSP126), moderate (SSP370) and extreme (SSP585) future emission trajectories) between two consecutive time periods (i.e., current–2055, and 2055–2085). By 2055, the potential distribution range of *B. ermanii* will expand under all three climate scenarios. The medium and high suitable areas will decline under SSP370 and SSP585 scenarios from 2055 to 2085. Moreover, under the three climate scenarios, the uppermost altitudes of low suitable habitat will rise to 2,329 m a.s.l., while the altitudes of medium and high suitable habitats will fall to 2,201 and 2,051 m a.s.l. by 2085, respectively. Warming promotes the expansion of *B. ermanii* distribution range in Changbai Mountain, and this expansion will be modified by precipitation as climate warming continues. This interaction between temperature and precipitation plays a significant role in shaping the potential distribution range of *B. ermanii* in the alpine treeline ecotone. This study reveals the link between environmental factors, habitat distribution, and species distribution in the alpine treeline ecotone, providing valuable insights into the impacts of climate change on high-elevation vegetation, and contributing to mountain biodiversity conservation and sustainable development.

1. Introduction

Climate change has had particularly severe consequences, leading to the loss of hundreds of native plant species (IPCC, 2022). Recent climate changes in mountainous regions have been more pronounced than in lowlands (Pepin et al., 2022). Alpine treeline ecotones are known to be particularly vulnerable and sensitive to climate warming (Körner, 2012). Numerous studies have observed that distributions of tree species in alpine treeline ecotones have shifted towards higher altitudes under climate change (Chhetri and Thai, 2019; Danby and Hik, 2007; Liang et al., 2016; Du et al., 2018; Arekhi et al., 2018). However, stable or downward shifts of the alpine treeline have also been found in some regions (Xu et al., 2020; Chhetri and Cairns, 2015; Kullman, 2007). The distribution shifts of alpine treeline species have important implications for species existence and ecosystem service in mountains under global climate change.

The distribution of plant species in alpine treeline ecotone is sensitive to climate changes, particularly increasing temperatures, which has a

significant impact on the ecological structure and function of treeline ecotones (Wang et al., 2019). Temperature is widely recognized as the dominant driver of plant species density (Mi et al., 2022; Deng et al., 2023) and treeline plant species upward shift (Shi et al., 2022). Warming has improved tree growth, leading to the expansion of treeline species into the adjacent tundra ecosystem (Kruse et al., 2023). For example, the alpine treeline in Taurus Mountains moved approximately 22–45 m upwards in response to climate warming from 1970 to 2013 (Arekhi et al., 2018). Furthermore, precipitation may also have an impact on the distribution of tree species in treeline ecotone (Hansson et al., 2023). Sigdel et al. (2018) observed that the alpine treelines in the Himalayas shifted upwards in response to climate warming, but the shift rates appeared to be mediated by spring precipitation. Recent studies also found that the growth of birch (*Betula utilis*) and alpine dwarf shrub *Cassiope fastigiate* in the Himalayas has been persistently limited by precipitation at their upper limits (Liang et al., 2014, 2015).

In addition to temperature and precipitation, local environmental conditions such as topography and soils also affect the distribution of tree species in the alpine treeline ecotone (Case and Duncan, 2014; Camarero et al., 2017). For example, topography is an important factor affecting the distribution of alpine plant species (Carmel and Kadmon, 1999). Previous study showed that the rate of plant encroachment in alpine tundra of the Changbai Mountain was higher at lower altitudes than at higher altitudes (Wu et al., 2018). The plant communities in the forest-tundra ecotone were found to vary with aspect and slope (Dearborn and Danby, 2017), and the number of tree seedlings at Subarctic alpine treelines varied with aspect (Kambo and Danby, 2018).

Previous studies have used a variety of methods to investigate treeline shift in response to climate change, including field plot surveys (Kambo and Danby, 2018), seedling recruitment (Frei et al., 2018), dendroecological techniques (Du et al., 2018), and remote sensing images (Chhetri and Thai, 2019; Zong et al., 2014). For example, Du et al. (2018) used state-of-the-art dendroecological approach to reconstruct long-term changes in the alpine treeline on Changbai Mountain, and found that the treeline species, *Betula ermanii* Cham., shifted upwards with climate warming. Zong et al. (2014) used RS and GIS to identify the tree locations and developed a logistic regression model using topographical variables to determine the main controls on tree locations. They found that aspect, wetness, and slope were the primary factors affecting tree locations on the west-facing slope of Changbai Mountain.

Modeling approach provides a valuable method for projecting future treeline dynamics and treeline movements (Tiwari et al., 2023). Species distribution models (SDMs) are commonly used statistical models that predict potential species distribution by integrating empirical data on species occurrences or abundance with data on relevant environmental factors (Anderson, 2017). Most previous studies have employed SDMs to model the potential distribution of species in response to climate change (Banerjee et al., 2019; Ahmad et al., 2020). However, few studies have investigated the effects of topographic changes on model predictions. The MaxEnt model combining bioclimatic and topographic variables predicts a decrease in the distribution of *Taiwania cryptomerioides* in China (Zhao et al., 2020), and a northward and westward shift of *Haloxylon* in Central Asia with global warming (Li et al., 2019). It is widely recognized that Biomod2 model is more reliable than using a single model to predict species distribution (Thuiller et al., 2009; Breiner et al., 2015). Biomod2 has been extensively applied to quantify geographical patterns of species distribution under future climates, providing valuable insights for future conservation efforts (Ren et al., 2016; Zhao et al., 2021; Ray et al., 2021).

Those methods mentioned above, although with different focuses, are all considered to be effective in analyzing fine- and large-scale movements of treelines, but they have limitations in detecting temporal variations in treeline movements (Norberg et al., 2019). Therefore, it is essential to select the most appropriate approach or model for a given study (Beaumont et al., 2016). Globally, the temperature-sensitive alpine treeline (Paulsen and Körner, 2014) has already shifted upwards with past warming and will continue to shift upwards beyond its current position with current warming (Parmesan and Yohe, 2003; Li et al., 2006; Harsch et al., 2009; Liang et al., 2011, 2016; Wielgolaski et al., 2017; Du et al., 2018, 2021). To better understand the link between climate change and distribution range expansion of trees in the alpine ecotone, we studied the potential distribution of the treeline species *B. ermanii* in the treeline ecotone under three climate change scenarios in Changbai Mountain. We used a GF-2 satellite image, along with bioclimatic and topographic variables, to develop an ensemble suitable habitat model based on the species distribution modeling algorithms in Biomod2. We hypothesize that: (i) the expansion and upward shift of *B. ermanii* in Changbai Mountain are caused by air warming rather than other environmental factors, and (ii) the effect of warming on those movements (i.e., distribution expansion and upward shift) will be influenced by regional precipitation patterns.

2. Materials and methods

2.1. Study area

The Changbai Mountain (41°41′49″ to 42°25′18″ N and 127°42′55″ to 128°16′48″ E) is a dormant volcano located in the northeastern China at the border to North Korea (Du et al., 2018). The prevailing climate is temperate continental, with annual precipitation ranging from 800 to 1, 800 mm, and the annual mean growing season (late May–late September) temperature from −7.3 to 4.9 °C (Du et al., 2018). There are four vertical spectra of vegetation zones including mixed Korean pine broad-leaved forests distributed from 740 to 1,100 m a.s.l., mountain coniferous forests from 1,100 to 1,700 m a.s.l., deciduous broad-leaved *B. ermanii* forests from 1,700 to 1,950 m a.s.l., and alpine tundra above 2,000 m a.s.l. (Yu et al., 2014; Jin et al., 2021). *B. ermanii* is the dominant tree species at the treeline ranging from 2,000 to 2,030 m a.s.l., where trees with a height of >3 m and canopy cover of >20% (Cong et al., 2022; Du et al., 2018). The distribution of *B. ermanii* is scattered above 2,030 m and can reach up to 2,200 m a.s.l. (Cong et al., 2018). The study area (41°53′–42°04′ N, 127°57′–128°13′ E) is located in the *B. ermanii* forests and tundra above 1,700 m a.s.l. Excluding Tianchi area in Changbai Mountain, with a total area of 383.17 km² (Fig. 1), which provided the opportunity to study the spatial distribution of *B. ermanii* trees.

2.2. Species occurrences

The occurrence data of *B. ermanii* trees in Changbai Mountain was obtained from a GF-2 satellite image with high resolution (0.8 m). The cloud-free image was acquired at the leaf senescence period (September 23, 2017). The GF-2 satellite data were preprocessed with radiance calibration, atmospheric correction, and image focus the ENVI5.3 (Jia et al., 2019). The *B. ermanii* distribution was obtained in study area using combined object-oriented classification and visual interpretation (Şerban et al., 2021). The *B. ermanii* distribution space was divided in 50 m × 50 m grid cells and randomly create one occurrence per grid cell to reduce sampling bias (Liu et al., 2019; Naudiyal et al., 2021). This procedure was repeated 5 times to generate 5 presence datasets. With the ArcGIS 10.2 (ESRI, Redlands, CA, USA), a sighting point map was developed.

2.3. Environmental data

We initially selected 24 environmental factors that may influence the distribution of *B. ermanii* to model the current species distribution patterns. These included 19 bioclimatic variables describing current (1979–2017) derived from monthly precipitation and monthly daily maximum, minimum and mean temperatures from CHELSA (https://chelsa-climate.org) with 30 arc sec spatial resolution (Karger et al., 2017) and 5 topographic attributes such as elevation, slope, aspect, topographic wetness index (TWI) and topographic relief (TR) derived from high resolution digital elevation model (DEM) with ArcGIS 10.2 (Table 1). The
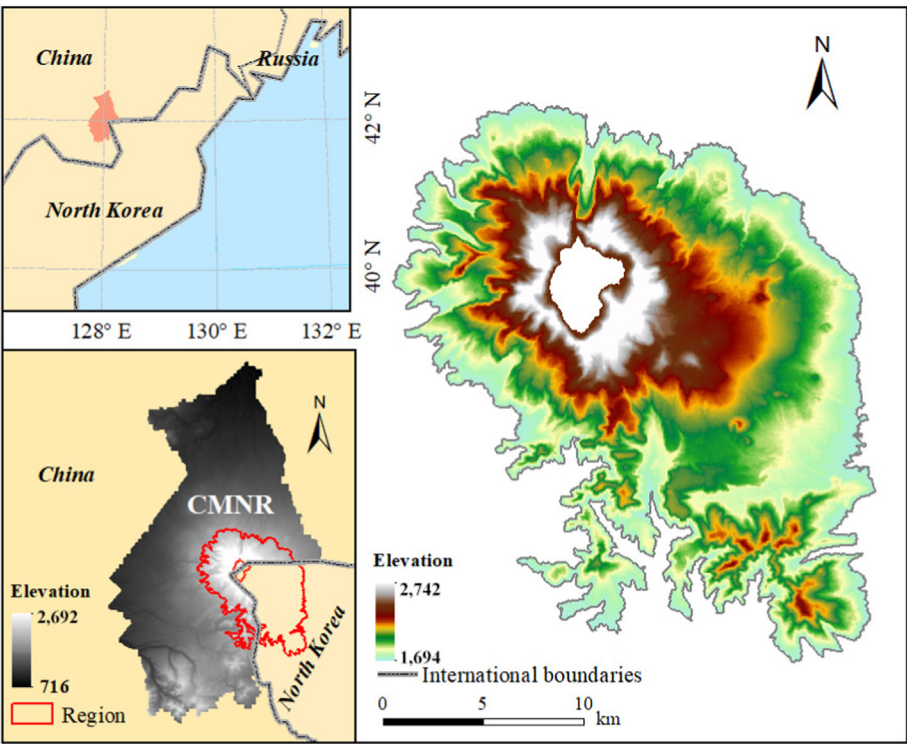
Fig. 1. Geographical location of the study area in the northeastern China at the border to North Korea and altitude distribution, CMNR represents the Changbai Mountain Nature Reserve.

DEM was derived from the PRISM (panchromatic remote-sensing instrument for stereo mapping) sensor attached to the ALOS (advanced land observing satellite). It had a spatial resolution of 5 m with a horizontal and vertical accuracy of 5 m. Future scenarios were downscaled GCMs (global climate model) data of 2055 (average for 2041–2070) and 2085 (average for 2071–2100) from CMIP6 under the shared socioeconomic pathways (SSPs) SSP126, SSP370, SSP585 scenarios released by IPCC Accessment Report 6 (AR6). These environmental parameters were all preprocessed to a general spatial resolution of 50 m latitude/longitude. The high resolution DEM was aggregated from 5 m to a coarser resolution of 50 m and the monthly precipitation was resampled to 50 m. The monthly daily maximum, minimum and mean temperatures were downscaled to 50 m by multiple linear regression (MLR) (Kostopoulou et al., 2007) with elevation, slope, aspect.

In order to remove variables of high redundancy, we used Pearson's correlation to examine the cross-correlation and removed highly correlated variables ($r > |0.90|$). Out of 24 variables, only 8 were selected as evaluator variables (Table 1). The temperature and precipitation change rate (TPR) between two consecutive time periods was calculated by the following equation:

Table 1
Environmental variables used for Biomod2 in this study.

Variables	Description	Unit
Bio05	Max temperature of warmest month	°C
Bio18	Precipitation of warmest quarter	mm
Bio19	Precipitation of coldest quarter	mm
Aspect	Direction normal to the slope projected onto the horizontal plane	–
Elevation	Height above sea level	m
Slope	Relative degree of steepness	°
TWI	Topographic wetness index $\ln\left(\frac{\alpha}{\tan\beta}\right)$ (Beven and Kirkby, 1979)	–
TR	Topographic relief $\text{Max}_{\text{Regional altitude}} - \text{Min}_{\text{Regional altitude}}$ (Niu and Harris, 1996)	–

$$\text{TPR}\% = \frac{\frac{T_{\text{gs}_{t_i}} - T_{\text{gs}_{t_0}}}{T_{\text{gs}_{t_0}}} - \frac{P_{\text{gs}_{t_i}} - P_{\text{gs}_{t_0}}}{P_{\text{gs}_{t_0}}}}{\frac{T_{\text{gs}_{t_i}} - T_{\text{gs}_{t_0}}}{T_{\text{gs}_{t_0}}}} \times 100\%$$

where T_{gs} is the growing-season temperature (°C), P_{gs} is the growing-season precipitation (mm), t_i and t_0 respesent the future time period and current climatic conditions, respectively.

In the future, it would be projected that the change rates of growing-season temperature (T_{gs}) would be greater than the change rates of growing-season precipitation (P_{gs}) between two consecutive time periods (i.e., current–2055, and 2055–2085) under three climate scenarios (Fig. 6g–l). From the current to 2055, the variations in the rate of temperature and precipitation changes under SSP126 was larger than those under SSP370 and SSP585 (Fig. 6g–i). However, under the 2085 scenario, the variations in the rate of temperature and precipitation changes appeared to increase with the future increasing greenhouse gas emissions scenarios than compared to 2055 scenario (Fig. 6j–l).

2.4. Species distribution models

To take into account the strengths and weaknesses of individual models, it may be safer to use an ensemble model (Shabani et al., 2016). The current and future habitat suitability of *B. ermanii* was predicted using the "biomod2" platform (Thuiller et al., 2009) in R (R Core Team, 2016) based on ten models belonging to different classes adopted: three regression models (generalized linear model, GLM; multivariate adaptive regression splines, MARS; and generalized additive models, GAM), five machine-learning models (artificial neural network, ANN; maximum entropy, MaxEnt; random forest, RF; and generalized boosting model, GBM; classification tree analysis, CTA), one classification model (flexible discriminant analysis, FDA) and a range envelope (surface range envelope, SRE).

We randomly selected 5,000 pseudo-absences and the process repeated five times. The models were trained using pseudo-absences falling from 100 to 1,000 m away from the presence to improve model

performance (Mainali et al., 2015). For each model, 80% data were used for calibrating model and the remaining 20% for validating the model (Liu et al., 2019). The performance of each model was evaluated through repeated 10 times data-splitting approach. The relative operating characteristic (ROC) (Lusted, 1984) and the true skill statistic (TSS) (Allouche et al., 2006) were used to calibrate and validate the robustness of evaluation for the models. The output values for ROC or TSS closer to 1 represent better models performance in prediction (Zhong et al., 2022). We retained these models with the following requirements: The TSS >0.65 (Alabia et al., 2016), ROC >0.75 (Rathore et al., 2019) and deviation comparing the *B. ermanii* distribution of current predicted and the *B. ermanii* distribution of current observed. We derived the averaged predictions of these models weighted by their TSS scores.

2.5. Data analysis

We used Biomod2 with eight variables and extracted occurrence data of *B. ermanii* in 2017 to project tree species distribution in 2055 and 2085 under SSP126, SSP370 and SSP585 scenarios. The model output results were categorized into three classes representing habitat suitability: low (25%–50%), medium (50%–75%) and high (>75%) probability of occurrence. Values below 25% were excluded as we indicated habitats that were deemed non-suitable habitat based on the logistic threshold (Chakraborty et al., 2016). To quantify the contributions of different variables in determining the distribution of *B. ermanii*, we used random forest model to obtain the relative importance. We analysed effects of time and climate change on changes in tree species distribution and their maximum altitudes. We calculated the relative differences in the distribution of *B. ermanii* between the current climate scenario and climate change scenarios during two consecutive time periods: current–2055 and 2055–2085. We also calculated the variations in the rate of temperature and precipitation changes between two consecutive time periods.

3. Results

3.1. Model validation

The current potential distribution of *B. ermanii* in the study area was found to be 130.22 km^2, almost twice the size of the observed distribution (Fig. 2a–c). However, the distribution of medium and high suitable habitats more closely matched the current observed distribution of *B. ermanii* in Changbai Mountain (Fig. 2a and b). Among the three suitable habitats, the proportion of low suitable habitat area in our study area was the highest at 17.43%, followed by high suitable habitat (8.70%) and

medium suitable habitat (7.85%) (Fig. 2c).

The performance of ten species distribution model (SDM) algorithms for predicting the potential distribution of *B. ermanii* under current climate conditions showed significant differences, as determined by the Kruskal-Wallis *H* test ($p < 0.001$) (Table 2). Among these models, machine-learning models including GBM, RF, CTA, and MaxEnt, demonstrated higher accuracy in modeling the suitable habitat of *B. ermanii*, with ROC mean scores ranging from 0.90 to 0.95 and TSS mean scores between 0.66 and 0.84. Notably, the potential distribution of *B. ermanii* predicted by these four models under current climate conditions closely matched the current observed distribution of *B. ermanii* (Fig. S1). Therefore, we utilized the Biomod2 platform with the GBM, CTA, RF, and MaxEnt modeling methods to simulate *B. ermanii* distribution.
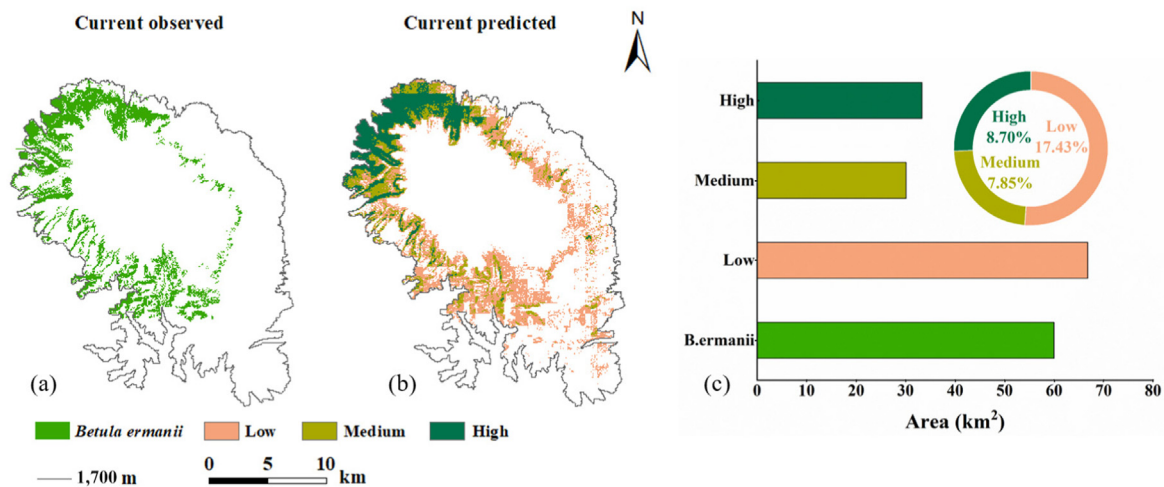
3.2. Importance of variables

Our analysis revealed that bioclimatic predictors had a greater impact on *B. ermanii* distribution compared to topographic variables (Fig. 3). Specifically, precipitation of the warmest quarter (Bio18, 27.96%), precipitation of the coldest quarter (Bio19, 17.40%), and maximum temperature of the warmest month (Bio05, 12.45%) made the greatest contributions to the distribution model for *B. ermanii* relative to other variables. These variables accounted for a significant proportion of the

Table 2
The performances (Mean ± SD) of ten species distribution models (SDM) for *Betula ermanii*. Relative operating characteristic (ROC) and true skill statistic (TSS) values are given.

SDM	ROC ± SD	TSS ± SD
GLM	0.911 ± 0.008	0.637 ± 0.019
GBM	**0.946 ± 0.007**	**0.747 ± 0.027**
GAM	0.918 ± 0.008	0.659 ± 0.029
CTA	**0.908 ± 0.008**	**0.760 ± 0.030**
ANN	0.793 ± 0.091	0.510 ± 0.129
SRE	0.722 ± 0.014	0.444 ± 0.029
FDA	0.858 ± 0.053	0.568 ± 0.109
MARS	0.918 ± 0.008	0.663 ± 0.026
RF	**0.973 ± 0.005**	**0.840 ± 0.023**
MaxEnt	**0.921 ± 0.009**	**0.667 ± 0.029**

Notes: generalized linear model (GLM), generalized boosting model (GBM), generalized additive models (GAM), classification tree analysis (CTA), artificial neural network (ANN), surface range envelope (SRE), flexible discriminant analysis (FDA), multivariate adaptive regression splines (MARS), random forest (RF), maximum entropy (MaxEnt).

Fig. 2. Relative importance of environment variables for the distribution of *Betula ermanii* in Changbai Mountain. The importance is based on the sum of weight derived from the random forest model.
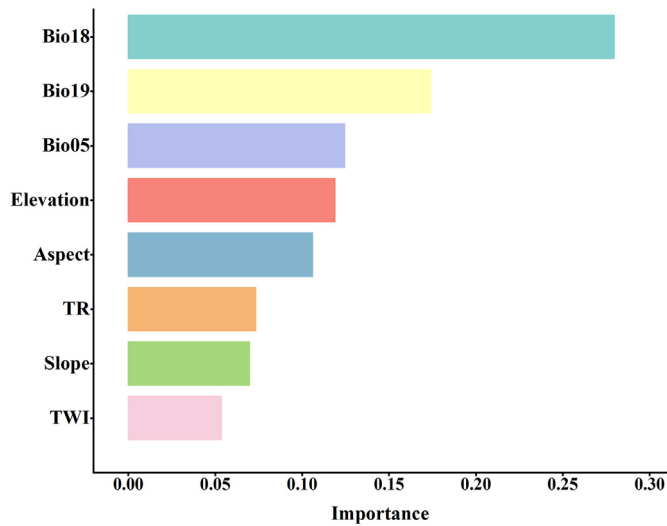
Fig. 3. Current observed (**a**) and current predicted (**b**) distribution for *B. ermanii* in Changbai Mountain, current observed areas and predicted suitable areas (**c**) for *B. ermanii* are categorized divided into low, medium, and high suitable habitats. The percentages represent the proportion of each suitable habitat area in the study area (the area above 1,700 m a.s.l. In Changbai Mountain excluding Tianchi area, with a total area of 383.17 km^2).

model, with cumulative contributions reaching as high as 62.4%. However, the contribution of topographic variables to the distribution of *B. ermanii* was relatively limited. Elevation and aspect were the most significant factors, together accounting for 22.3% of the variation in *B. ermanii* distribution among the topographic variables. In contrast, topographic relief, slope and topographic wetness index played minor roles contributing less than 10%.

3.3. Changes in future potential distributions

It was observed that all three suitable habitat areas would increase under future climate scenarios in both 2055 and 2085 compared with the current scenario (Fig. 4a–h). Moreover, the potential distribution percentage of *B. ermanii* in 2055 increased by 30%, 35%, 9%, respectively, under the three climate scenarios (SSP126, SSP370, SSP585) (Fig. 4d). Compared with the two future periods, by 2085, the distribution of *B. ermanii* in both medium and high suitable areas expanded under SSP126 scenario, but these areas showed a trend of retreat under the SSP370 and SSP585 scenarios (Fig. 4d and h). Both time periods and scenarios, and their interaction had significant effects on the maximum altitudes of *B. ermanii* distribution (Fig. 5a–c). Moreover, the maximum altitudes varied significantly with time periods and classes (habitat suitability) and their interaction (Table 3). Among three scenarios, the maximum altitudes of three suitable habitats under SSP370 were highest except for the high suitable habitat in 2085 (Fig. 5a–c). Furthermore, the maximum altitudes of three suitable habitats under SSP585 scenarios in both 2055 and 2085 would decrease significantly compared to the SSP126 scenarios (Fig. 5a–c). In future, the maximum altitudes for suitable habitats are expected to range between 2,245 and 2,388 m for low suitable habitat, 2,133 and 2,366 m for medium suitable habitat and 2,013 and 2,236 m for high suitable habitat, respectively (Fig. 5a–c). Additionally, the maximum altitudes of low suitable habitats in 2085 would be higher than in 2055 under three future scenarios (Fig. 5a), but the opposite patterns were observed for the maximum altitudes of medium and high suitable habitats (Fig. 5c).

Compared to the current scenario, the occurrence probability of *B. ermanii* would significantly increase at high altitudes under SSP126 and SSP370-2055 climate scenarios, but decreased on the north and south sides of the Changbai Mountain under SSP585-2055 climate scenario (Fig. 6a–c). Conversely, under the 2085 scenario, the increased habitats were at low elevations, but large amounts of habitats decreased under three climate scenarios compared to 2055 (Fig. 6d–f). Additionally, the regions where the probability of *B. ermanii* occurrence were
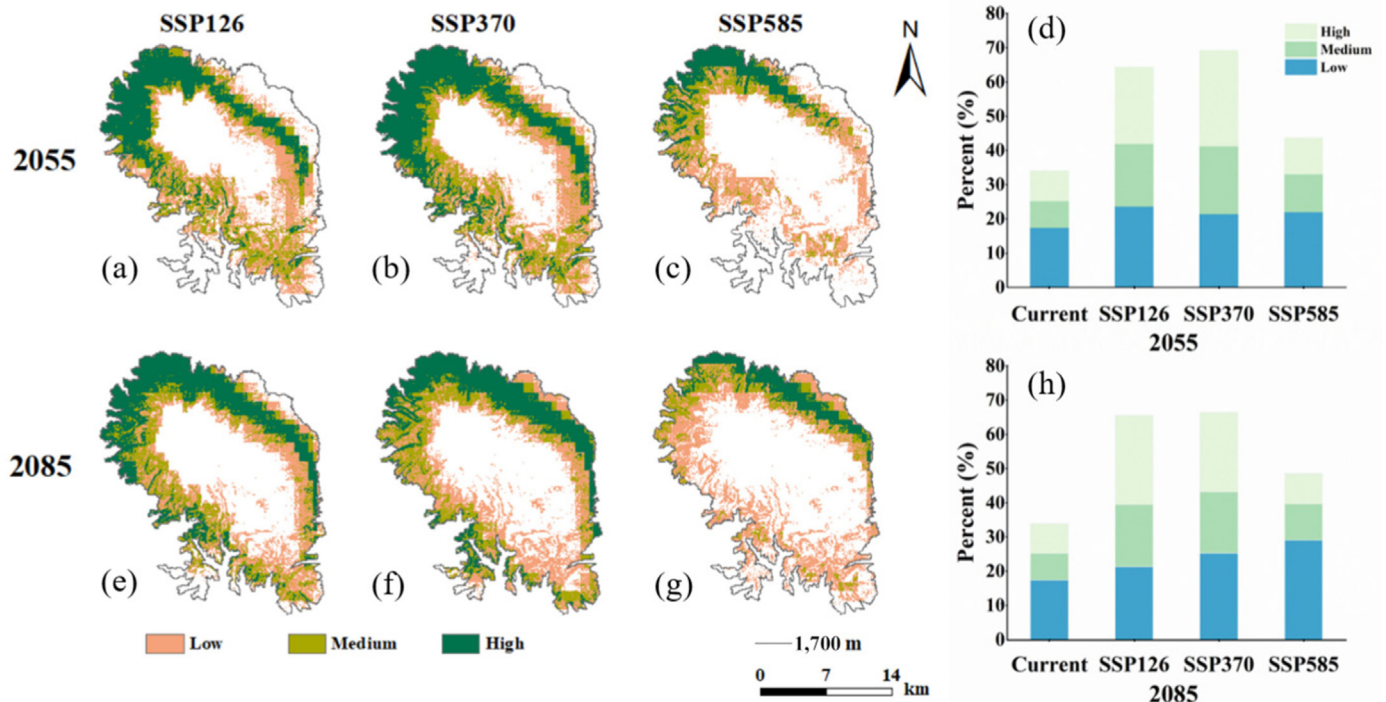
Fig. 4. Future species distribution of *B. ermanii* under climate change scenarios SSP126, SSP370 and SSP585 in 2055 (**a**, **b**, **c**) and 2085 (**e**, **f**, **g**). The percentages represent the proportion of each suitable habitat area (low, medium, and high) in the study area under current and climate change scenarios SSP126, SSP370 and SSP585 in 2055 (**d**) and 2085 (**h**).
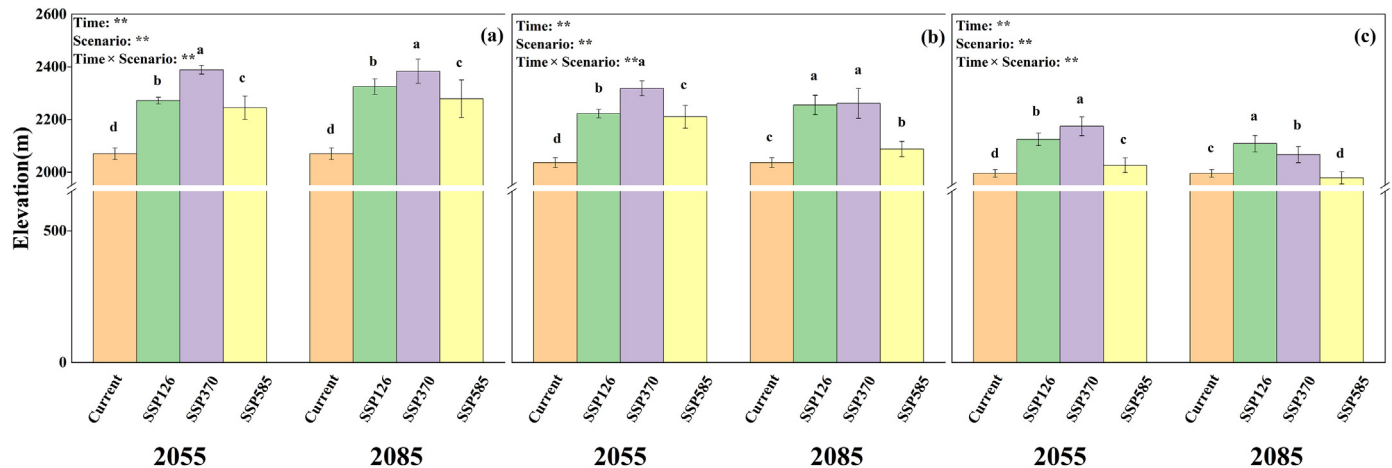
Fig. 5. Maximum altitudes (Mean ± SD) of *B. ermanii* distribution under current and climate change scenarios SSP126, SSP370 and SSP 585 in low (**a**), medium (**b**), and high (**c**) suitable habitats in 2055 and 2085, respectively. Different lowercase letters indicate significant differences ($p < 0.05$) among current and climate change scenarios SSP126, SSP370 and SSP585, as determined by Tukey's HSD test. **indicates significant differences ($p < 0.01$) of time periods, scenarios, and their interactions on the maximum altitude of *B. ermanii*, tested with two-way nested ANOVA.

Table 3

Effects of time periods, classes (habitat suitability), and their interactions on the maximum altitude of *B. ermanii*, tested with two-way nested ANOVA. *F* and *p* values are given.

Factors	Df	Maximum altitude	
		F	*p*
Time periods	1	255.94	< 0.001
Classes	2	6,975.19	< 0.001
Time periods × Classes	2	267.04	< 0.001

expected to decrease mainly located in non-suitable and low suitable habitats.

4. Discussion

Our results showed significant differences in the performance of ten SDMs algorithms for potential distribution of *B. ermanii* under current climate conditions. This was consistent with Iverson and McKenzie's (2013) findings that, although climate modeling played an important role in understanding the impacts of climate change on plants, the performance of different climate models varied significantly, as noted by Cheaib et al. (2012). Moreover, we found that the machine-learning models (i.e., GBM, RF, CTA and MaxEnt) were the best individual models with higher ROC and TSS values, which was consistent with previous researches (An et al., 2018; Garris et al., 2015; Morera et al., 2021; Valavi et al., 2022). Therefore, we utilized the Biomod2 platform with these four models to predict the potential distribution of *B. ermanii*. Our model indicated that the current predicted distribution of *B. ermanii* was primarily aggregated on the northern and western slopes of the Changbai Mountain (Fig. 2a and b), which corresponded to the observed reality, but appeared larger than the current observed (Fig. 2c). The medium and high suitable habitats, however, aligned with the observed distribution, thus we considered these as the most suitable for *B. ermanii*.

Overall, the model results showed that the possibility of *B. ermanii* distribution increased under low and medium greenhouse gas emissions scenarios (SSP126, SSP370), but decreased significantly under the high greenhouse gas emissions scenario (SSP585) (Fig. 4a–h). This finding consisted with the previous study by Hu et al. (2015) who found that the *Platycladus orientalis* distribution would increase under RCP2.6 but appeared to decrease under RCP8.5. Additionally, the maximum altitudes of medium and high suitable habitats for *B. ermanii* in the current scenario were 2,072 and 2,020 m, respectively, which was in agreement

with the reported upper elevational limit of *B. ermanii*'s in Changbai Mountain (Du et al., 2018). However, slight upward shifts in the maximum altitudes of *B. ermanii* had been observed in both medium and high suitable habitats under three future climate scenarios except for SSP585-2085 compared with the current scenario (Fig. 5a–c). This trend was consistent with previous study (Du et al., 2018), which indicated that an upward shift in the upper limits of *B. ermanii* in response to recent warming. Furthermore, previous research affirmed that the timberline of *B. ermanii* is located at about 2,200 m on the northern slope of Changbai Mountain from 1400 a B.P. to 920 a B.P. (Guo et al., 2012). This supports that *B. ermanii* in Changbai Mountain will continue to shift upward with future warming.

Temperature is an important driving factor for increasing tree growth and recruitment in recent decades. Warming can improve the plant physiology and ecophysiology, thereby facilitating tree recruitment. Numerous studies have shown that species' spatial distributions expanded to high altitudes significantly in response to climate warming (Chen et al., 2011; Li et al., 2019; Sun et al., 2020). For example, recent warming had driven the upward migration of *B. ermanii* in Changbai Mountain (Du et al., 2018). Similarly, the occurrence probabilities of six allelopathic flowering plants from North America increased under climate change scenarios (Wang et al., 2022). Thus, temperature is a key factor limiting tree growth, especially for alpine treeline tree species (Liang et al., 2016; Gou et al., 2012). However, previous studies showed that the suitable habitat areas would slightly decrease with climate warming, indicating that continuous rise in temperature could may even have a negative impact on plant growth (Hu et al., 2015; Naudiyal et al., 2021). Consistently, our predictions showed that the occurrence probabilities of *B. ermanii* tended to increase in the majority of the study area under three climate scenarios by 2055 compared to current scenario (Fig. 6a–c), but may decrease under future climate scenarios from 2055 to 2085 (Fig. 6d–f). Our analysis also revealed that an increase in temperature will result in more suitable habitats (Fig. 6g–i). However, a decline in suitable habitats can be attributed to an inadequate increase in precipitation compared to rising temperatures (Fig. 6j–l).

Warmer temperatures at treeline ecotones could potentially result in a deficit of soil moisture due to elevated evapotranspiration (Trujillo et al., 2012). Our study's findings indicated that precipitation and temperature were the key factors in the spatial distribution of *B. ermanii* (Fig. 3). Furthermore, the occurrence probability of *B. ermanii* reduction increased with decreasing precipitation (Fig. S2), aligning with observations by Reich et al. (2018), who found that positive effects of climate warming on tree growth in southern boreal forests may become negative when transitioning from rainy to modestly dry periods during the
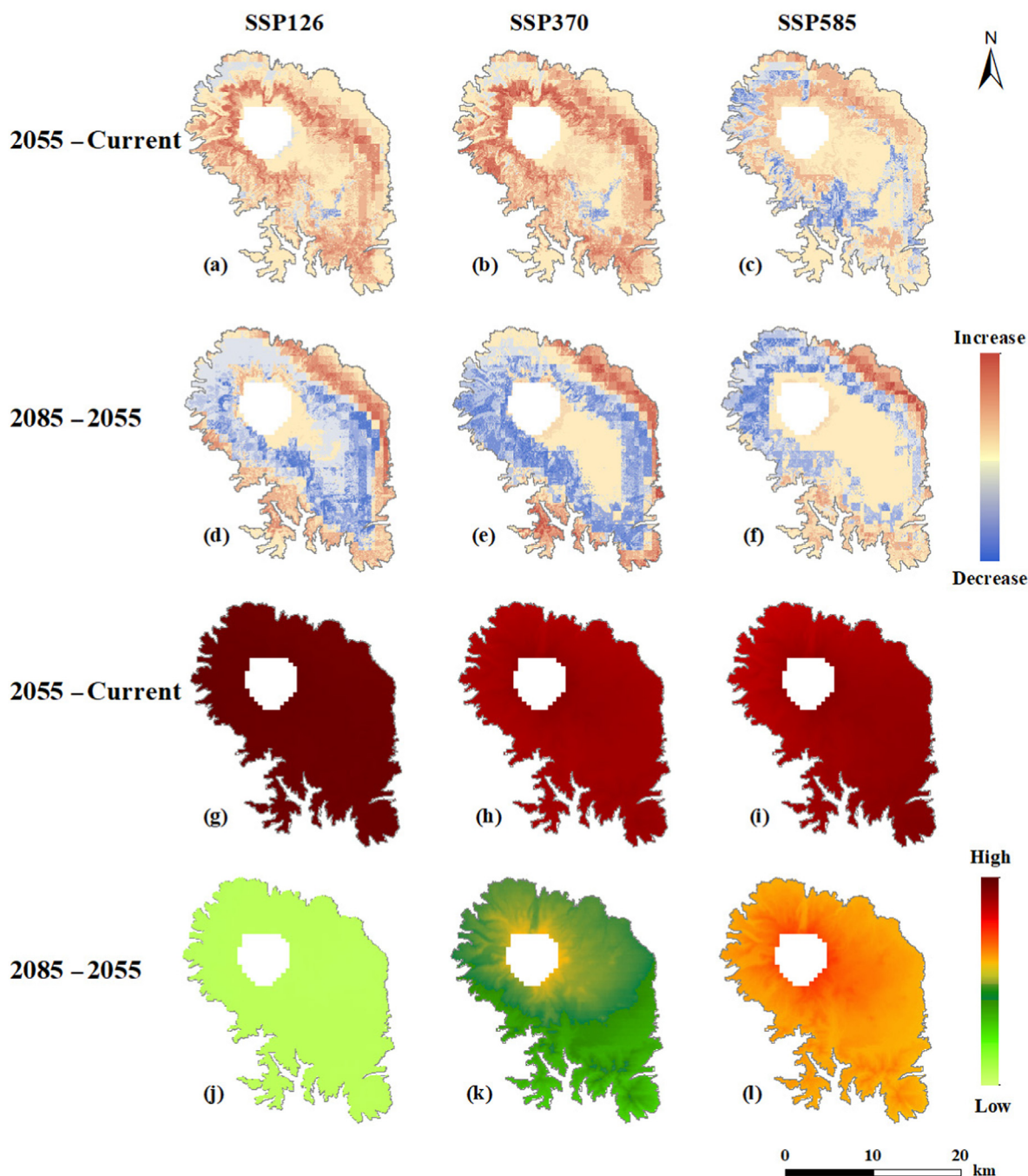
Fig. 6. Dynamics changes in the distribution of *B. ermanii* between the current and climate change scenarios SSP126, SSP370 and SSP585 between two consecutive time periods: 2055–current (**a**, **b**, **c**) and 2085–2055 (**d**, **e**, **f**). Variations in the rate of temperature and precipitation changes between two consecutive time periods: 2055–current (**g**, **h**, **i**) and 2085–2055 (**j**, **k**, **l**). Color gradients represent the variables broken into their respective percentile classes for the magnitude of the distributional and environmental changes between scenarios. (For interpretation of the references to colour in this figure legend, the reader is referred to the Web version of this article.)

growing season. Another study showed that radial growth of Erman's birch was significantly affected by precipitation in Changbai Mountain (Yu et al., 2007). Similarly, water deficits in August reduced growth of tree species of an altitudinal ecotone on Mount Norikura, central Japan, regardless of their upper or lower distribution limits (Takahashi et al., 2003). In contrast, Wang et al. (2018) found *B. ermanii* populations were more sensitive to air temperature variations than to changes in precipitation. These suggest that long-term tree species distribution was primarily constrained by temperature, highlighting the need to consider the influence of precipitation when assessing the impacts of climate warming on tree species distribution.

A number of other factors not considered in this study may contribute to uncertainty in our projections. We only simulated the effects of climate change and topographic variables on the future distribution of treeline trees. We identified temperature and precipitation as the primary climatic factors affecting tree species, without considering nitrogen deposition and CO_2 fertilization, which can also significantly impact tree species distributions. In addition, the climate variables were initially at a spatial resolution of 1 km, however, they have been downscaled to 50 m and validated with growing season temperature between 2015 and 2017 from Wang et al. (2019), achieving an RMSE of 0.94 and an R^2 of 0.90. Coarser climate resolution data (i.e. 30 arc sec ~1 km) has been applied

in previous studies to well predict future vegetation distribution at regional scales (Guo et al., 2018; Queirós et al., 2020). Moreover, it has been suggested that, at regional scales, the use of coarse spatial resolution data in SDMs can enhance models accuracy and preserve details (Pineda and Lobo, 2012). Despite such limitation, there are good reasons to believe that our approach effectively assesses how climate change and topographic variables interact to affect tree species distributions. Bimod2 has been shown in previous studies to well capture forest distribution and stand dynamics (Ren et al., 2016; Chakraborty et al., 2021; Queirós et al., 2020).

5. Conclusion

This study reveals the link between environmental factors including temperature and precipitation, habitat distribution, and species distribution in the alpine treeline ecotone. Consistent with our 1st hypothesis, we find that climate warming promotes the expansion and upward shift of the distribution *B. ermanii* in the alpine ecotone of the Changbai Mountain, but these warming effects are influenced by precipitation, which is consistent with our 2nd hypothesis. Such climate change-induced expansion of the distribution range of treeline trees will inevitably lead to changes in species composition, community structure and biodiversity, and further affect ecosystem service within and beyond the alpine treeline ecotone on high mountains. Therefore, the present study provides valuable insights into the impacts of climate change on high-mountain vegetation, contributing to mountain biodiversity conservation and sustainable development.

Data availability

For manuscripts that are accepted, all authors agree to make data and materials available to third party academic researchers upon reasonable request.

CRediT authorship contribution statement

Yu Cong: Methodology, Conceptualization, Funding acquisition. **Yongfeng Gu:** Data curation, Formal analysis, Software. **Wen J. Wang:** Software, Validation, Visualization. **Lei Wang:** Validation, Software, Visualization. **Zhenshan Xue:** Validation, Software, Visualization. **Yingyi Chen:** Software, Validation, Visualization. **Yinghua Jin:** Resources, Conceptualization, Supervision. **Jiawei Xu:** Writing – review & editing. **Mai-He Li:** Writing – review & editing. **Hong S. He:** Writing – review & editing. **Ming Jiang:** Writing – review & editing.

Declaration of competing interest

The authors declared that they have no conflicts of interest to this work. We declared that we did not have any commercial or associative interest that represented a conflict of interest in connection with the work submitted.

Appendix A. Supplementary data

Supplementary data to this article can be found online at https://doi.org/10.1016/j.fecs.2024.100166.

References

Ahmad, S., Yang, L., Khan, T.U., Wanghe, K., Li, M., Luan, X., 2020. Using an ensemble modelling approach to predict the potential distribution of Himalayan gray goral (*Naemorhedus goral bedfordi*) in Pakistan. Glob. Ecol. Conserv. 21, e00845. https://doi.org/10.1016/j.gecco.2019.e00845.

Alabia, I.D., Saitoh, S.-I., Igarashi, H., Ishikawa, Y., Usui, N., Kamachi, M., Awaji, T., Seito, M., 2016. Ensemble squid habitat model using three-dimensional ocean data. ICES J. Mar. Sci. 73 (7), 1863–1874. https://doi.org/10.1093/icesjms/fsw075.

Allouche, O., Tsoar, A., Kadmon, R., 2006. Assessing the accuracy of species distribution models: prevalence, kappa and the true skill statistic (TSS). J. Appl. Ecol. 43 (6), 1223–1232. https://doi.org/10.1111/j.1365-2664.2006.01214.x.

An, A., Zhang, Y., Cao, L., Jia, Q., Wang, X., 2018. A potential distribution map of wintering Swan Goose (*Anser cygnoides*) in the middle and lower Yangtze River floodplain, China. Avian Res. 9, 43. https://doi.org/10.1186/s40657-018-0134-5.

Anderson, R.P., 2017. When and how should biotic interactions be considered in models of species niches and distributions? J. Biogeogr. 44 (1), 8–17. https://doi.org/10.1111/jbi.12825.

Arekhi, M., Yesil, A., Ozkan, U.Y., Balik Sanli, F., 2018. Detecting treeline dynamics in response to climate warming using forest stand maps and Landsat data in a temperate forest. For. Ecosyst. 5, 23. https://doi.org/10.1186/s40663-018-0141-3.

Banerjee, A.K., Mukherjee, A., Guo, W., Ng, W.L., Huang, Y., 2019. Combining ecological niche modeling with genetic lineage information to predict potential distribution of *Mikania micrantha* Kunth in South and Southeast Asia under predicted climate change. Glob. Ecol. Conserv. 20, e00800. https://doi.org/10.1016/j.gecco.2019.e00800.

Beaumont, L.J., Graham, E., Duursma, D.E., Wilson, P.D., Cabrelli, A., Baumgartner, J.B., Hallgren, W., Esperón-Rodríguez, M., Nipperess, D.A., Warren, D.L., Laffan, S.W., VanDerWal, J., 2016. Which species distribution models are more (or less) likely to project broad-scale, climate-induced shifts in species ranges? Ecol. Model. 342, 135–146. https://doi.org/10.1016/j.ecolmodel.2016.10.004.

Beven, K.J., Kirkby, M.J., 1979. A physically based, variable contributing area model of basin hydrology/Un modèle à base physique de zone d'appel variable de l'hydrologie du bassin versant. Hydrol. Sci. J. 24 (1), 43–69. https://doi.org/10.1080/02626667909491834.

Breiner, F.T., Guisan, A., Bergamini, A., Nobis, M.P., 2015. Overcoming limitations of modelling rare species by using ensembles of small models. Methods Ecol. Evol. 6 (10), 1210–1218. https://doi.org/10.1111/2041-210X.12403.

Camarero, J.J., Linares, J.C., García-Cervigón, A.I., Batllori, E., Martínez, I., Gutiérrez, E., 2017. Back to the future: the responses of alpine treelines to climate warming are constrained by the current ecotone structure. Ecosystems 20, 683–700. https://doi.org/10.1007/s10021-016-0046-3.

Carmel, Y., Kadmon, R., 1999. Effects of grazing and topography on long-term vegetation changes in a Mediterranean ecosystem in Israel. Plant Ecol. 145, 243–254. https://doi.org/10.1023/A:1009872306093.

Case, B.S., Duncan, R.P., 2014. A novel framework for disentangling the scale-dependent influences of abiotic factors on alpine treeline position. Ecography 37 (9), 838–851. https://doi.org/10.1111/ecog.00280.

Chakraborty, A., Joshi, P., Sachdeva, K., 2016. Predicting distribution of major forest tree species to potential impacts of climate change in the central Himalayan region. Ecol. Eng. 97, 593–609. https://doi.org/10.1016/j.ecoleng.2016.10.006.

Chakraborty, D., Móricz, N., Rasztovits, E., Dobor, L., Schueler, S., 2021. Provisioning forest and conservation science with high-resolution predicted distribution of major European tree species under climate change. Ann. For. Sci. 78 (2), 1–18. https://doi.org/10.1007/s13595-021-01029-4.

Cheaib, A., Badeau, V., Boe, J., Chuine, I., Delire, C., Dufrêne, E., François, C., Gritti, E.S., Legay, M., Pagé, C., 2012. Climate change impacts on tree ranges: model intercomparison facilitates understanding and quantification of uncertainty. Ecol. Lett. 15 (6), 533–544. https://doi.org/10.1111/j.1461-0248.2012.01764.x.

Chen, I.-C., Hill, J.K., Ohlemüller, R., Roy, D.B., Thomas, C.D., 2011. Rapid range shifts of species associated with high levels of climate warming. Science 333 (6045), 1024–1026. https://doi.org/10.1126/science.1206432.

Chhetri, P.K., Cairns, D.M., 2015. Contemporary and historic population structure of *Abies spectabilis* at treeline in Barun valley, eastern Nepal Himalaya. J. Mt. Sci. 12, 558–570. https://doi.org/10.1007/s11629-015-3454-5.

Chhetri, P.K., Thai, E., 2019. Remote sensing and geographic information systems techniques in studies on treeline ecotone dynamics. J. For. Res. 30, 1543–1553. https://doi.org/10.1007/s11676-019-00897-x.

Cong, Y., Saurer, M., Bai, E., Siegwolf, R., Gessler, A., Liu, K., Han, H., Dang, Y., Xu, W., He, H.S., 2022. In situ $^{13}CO_2$ labeling reveals that alpine treeline trees allocate less photoassimilates to roots compared with low-elevation trees. Tree Physiol. 42, 1943–1956. https://doi.org/10.1093/treephys/tpac048.

Cong, Y., Wang, A., He, H.S., Yu, F.-H., Tognetti, R., Cherubini, P., Wang, X., Li, M.-H., 2018. Evergreen *Quercus aquifolioides* remobilizes more soluble carbon components

but less N and P from leaves to shoots than deciduous *Betula ermanii* at the end-season. iForest 11 (4), 517–525. https://doi.org/10.3832/ifor2633-011.

Danby, R.K., Hik, D.S., 2007. Variability, contingency and rapid change in recent subarctic alpine tree line dynamics. J. Ecol. 95, 352–363. https://doi.org/10.1111/j.1365-2745.2006.01200.x.

Dearborn, K.D., Danby, R.K., 2017. Aspect and slope influence plant community composition more than elevation across forest–tundra ecotones in subarctic Canada. J. Veg. Sci. 28, 595–604. https://doi.org/10.1111/jvs.12521.

Deng, J., Fang, S., Fang, X., Jin, Y., Kuang, Y., Lin, F., Liu, J., Ma, J., Nie, Y., Ouyang, S., Ren, J., Tie, L., Tang, S., Tan, X., Wang, X., Fan, Z., Wang, Q., Wang, H., Liu, C., 2023. Forest understory vegetation study: current status and future trends. For. Res. 3, 6. https://doi.org/10.48130/FR-2023-0006.

Du, H., Liu, J., Li, M.H., Büntgen, U., Yang, Y., Wang, L., Wu, Z., He, H.S., 2018. Warming-induced upward migration of the alpine treeline in the Changbai Mountains, northeast China. Global Change Biol. 24, 1256–1266. https://doi.org/10.1111/gcb.13963.

Du, H., Li, M.-H., Rixen, C., Zong, S., Stambaugh, M., Huang, L., He, H.S., Wu, Z., 2021. Sensitivity of recruitment and growth of alpine treeline birch to elevated temperature. Agric. For. Meteorol. 304–305, 108403. https://doi.org/10.1016/j.agrformet.2021.108403.

Frei, E.R., Bianchi, E., Bernareggi, G., Bebi, P., Dawes, M.A., Brown, C.D., Trant, A.J., Mamet, S.D., Rixen, C., 2018. Biotic and abiotic drivers of tree seedling recruitment across an alpine treeline ecotone. Sci. Rep. 8, 10894. https://doi.org/10.1038/s41598-018-28808-w.

Garris, H.W., Mitchell, R.J., Fraser, L.H., Barrett, L.R., 2015. Forecasting climate change impacts on the distribution of wetland habitat in the Midwestern United States. Global Change Biol. 21, 766–776. https://doi.org/10.1111/gcb.12748.

Gou, X., Zhang, F., Deng, Y., Ettl, G.J., Yang, M., Gao, L., Fang, K., 2012. Patterns and dynamics of tree-line response to climate change in the eastern Qilian Mountains, northwestern China. Dendrochronologia 30, 121–126. https://doi.org/10.1016/j.dendro.2011.05.002.

Guo, M., Wu, F., Huang, Y., Wang, L., Jie, D., 2012. Timberline transition and climatic variation recorded by phytolith assemblages from the Northern slope of Changbai mountains over the last 1.4 ka. Adv. Geosci. 2, 16–23. doi:10.4236/ag.2012.21002 (in Chinese).

Guo, Y., Li, X., Zhao, Z., Wei, H., 2018. Modeling the distribution of *Populus euphratica* in the Heihe River Basin, an inland river basin in an arid region of China. Sci. China Earth Sci. 61, 1669–1684. https://doi.org/10.1007/s11430-017-9241-2.

Hansson, A., Shulmeister, J., Dargusch, P., Hill, G., 2023. A review of factors controlling Southern Hemisphere treelines and the implications of climate change on future treeline dynamics. Agric. For. Meteorol. 332, 109375. https://doi.org/10.1016/j.agrformet.2023.109375.

Harsch, M.A., Hulme, P.E., McGlone, M.S., Duncan, R.P., 2009. Are treelines advancing? A global meta-analysis of treeline response to climate warming. Ecol. Lett. 12 (10), 1040–1049. https://doi.org/10.1111/j.1461-0248.2009.01355.x.

Hu, X.-G., Jin, Y., Wang, X.-R., Mao, J.-F., Li, Y., 2015. Predicting impacts of future climate change on the distribution of the widespread conifer *Platycladus orientalis*. PLoS One 10, e0132326. https://doi.org/10.1371/journal.pone.0132326.

IPCC, 2022. Synthesis Report of the IPCC Sixth Assessment Report (AR6). IPCC AR6 SYR. Interlaken, Switzerland. https://report.ipcc.ch/ar6syr/pdf/IPCC_AR6_SYR_LongerReport.pdf (Accessed 28 April 2022).

Iverson, L.R., McKenzie, D., 2013. Tree-species range shifts in a changing climate: detecting, modeling, assisting. Landsc. Ecol. 28, 879–889. https://doi.org/10.1007/s10980-013-9885-x.

Jia, K., Liu, J., Tu, Y., Li, Q., Sun, Z., Wei, X., Yao, Y., Zhang, X., 2019. Land use and land cover classification using Chinese GF-2 multispectral data in a region of the North China Plain. Front. Earth Sci. 13, 327–335. https://doi.org/10.1007/s11707-018-0734-8.

Jin, Y., Xu, J., He, H., Tao, Y., Wang, H., Zhang, Y., Hu, R., Gao, X., Bai, Y., Zhao, C., 2021. Effects of catastrophic wind disturbance on formation of forest patch mosaic structure on the western and southern slopes of Changbai Mountain. For. Ecol. Manag. 481, 118746. https://doi.org/10.1016/j.foreco.2020.118746.

Kambo, D., Danby, R.K., 2018. Factors influencing the establishment and growth of tree seedlings at Subarctic alpine treelines. Ecosphere 9, e02176. https://doi.org/10.1002/ecs2.2176.

Karger, D., Conrad, O., Böhner, J., Kawohl, T., Kreft, H., Soria-Auza, R., Zimmermann, N., Linder, H., Kessler, M., 2017. Climatologies at high resolution for the earth's land surface areas. Sci. Data 4, 170122. https://doi.org/10.1038/sdata.2017.122, 2017.

Kruse, S., Shevtsova, I., Heim, B., Pestryakova, L.A., Zakharov, E.S., Herzschuh, U., 2023. Tundra conservation challenged by forest expansion in a complex mountainous treeline ecotone as revealed by spatially explicit tree aboveground biomass modeling. Arctic Antarct. Alpine Res. 55 (1), 2220208. https://doi.org/10.1080/15230430.2023.2220208.

Körner, C., 2012. Alpine treelines: functional ecology of the global high elevation tree limits. Springer, Basel. https://doi.org/10.1657/1938-4246.46.1.292.

Kostopoulou, E., Giannakopoulos, C., Anagnostopoulou, C., Tolika, K., Maheras, P., Vafiadis, M., Founda, D., 2007. Simulating maximum and minimum temperature over Greece: a comparison of three downscaling techniques. Theor. Appl. Climatol. 90, 65–82. doi:10.1007/s00704-006-0269-x.

Kullman, L., 2007. Tree line population monitoring of *Pinus sylvestris* in the Swedish Scandes, 1973–2005: implications for tree line theory and climate change ecology. J. Ecol. 95, 41–52. https://doi.org/10.1111/j.1365-2745.2006.01190.x.

Li, J., Chang, H., Liu, T., Zhang, C., 2019. The potential geographical distribution of Haloxylon across Central Asia under climate change in the 21st century. Agric. For. Meteorol. 275, 243–254. https://doi.org/10.1016/j.agrformet.2019.05.027.

Li, M.H., Kräuchi, N., Gao, S.P., 2006. Global warming: can existing reserves really preserve current levels of biological diversity? J. Integr. Plant Biol. 48 (3), 255–259. https://doi.org/10.1111/j.1744-7909.2006.00232.x.

Liang, E., Wang, Y., Eckstein, D., Luo, T., 2011. Little change in the fir tree-line position on the southeastern Tibetan Plateau after 200 years of warming. New Phytol. 190 (3), 760–769. https://doi.org/10.1111/j.1469-8137.2010.03623.x.

Liang, E., Dawadi, B., Pederson, N., Eckstein, D., 2014. Is the growth of birch at the upper timberline in the Himalayas limited by moisture or by temperature? Ecology 95, 2453–2465. https://doi.org/10.1890/13-1904.1.

Liang, E., Liu, W., Ren, P., Dawadi, B., Eckstein, D., 2015. The alpine dwarf shrub *Cassiope fastigiata* in the Himalayas: does it reflect site-specific climatic signals in its annual growth rings? Trees 29, 79–86. https://doi.org/10.1007/s00468-014-1128-5.

Liang, E., Wang, Y., Piao, S., Lu, X., Camarero, J.J., Zhu, H., Zhu, L., Ellison, A.M., Ciais, P., Peñuelas, J., 2016. Species interactions slow warming-induced upward shifts of treelines on the Tibetan Plateau. Proc. Natl. Acad. Sci. U.S.A. 113, 4380–4385. https://doi.org/10.1073/pnas.1520582113.

Liu, C., Comte, L., Xian, W., Chen, Y., Olden, J.D., 2019. Current and projected future risks of freshwater fish invasions in China. Ecography 42, 2074–2083. https://doi.org/10.1111/ecog.04665.

Lusted, L.B., 1984. ROC Recollected. Sage Publications Sage CA, Thousand Oaks, CA.

Mainali, K.P., Warren, D.L., Dhileepan, K., McConnachie, A., Strathie, L., Hassan, G., Karki, D., Shrestha, B.B., Parmesan, C., 2015. Projecting future expansion of invasive species: comparing and improving methodologies for species distribution modeling. Global Change Biol. 21, 4464–4480. https://doi.org/10.1111/gcb.13038.

Mi, J., Ou, J., Liu, H., Shi, J., Chen, D., Bai, Y., 2022. The loss of plant species diversity dominated by temperature promotes local productivity in the steppe of eastern Inner Mongolia. Ecol. Indicat. 139, 108953. https://doi.org/10.1016/j.ecolind.2022.108953.

Morera, A., de Aragón, J.M., Bonet, J.A., Liang, J., De-Miguel, S., 2021. Performance of statistical and machine learning-based methods for predicting biogeographical patterns of fungal productivity in forest ecosystems. For. Ecosyst. 8, 21. https://doi.org/10.1186/s40663-021-00297-w.

Naudiyal, N., Wang, J., Ning, W., Gaire, N.P., Peili, S., Wei, Y., He, J., Ning, S., 2021. Potential distribution of *Abies*, *Picea*, and *Juniperus* species in the sub-alpine forest of Minjiang headwater region under current and future climate scenarios and its implications on ecosystem services supply. Ecol. Indicat. 121, 107131. https://doi.org/10.1016/j.ecolind.2020.107131.

Niu, W.-Y., Harris, W.M., 1996. China: the forecast of its environmental situation in the 21st century. J. For. Environ. 47, 101–114. doi:10.1006/jema.1996.0039.

Norberg, A., Abrego, N., Blanchet, F.G., Adler, F.R., Anderson, B.J., Anttila, J., Araújo, M.B., Dallas, T., Dunson, D., Elith, J., 2019. A comprehensive evaluation of predictive performance of 33 species distribution models at species and community levels. Ecol. Monogr. 89, e01370. https://doi.org/10.1002/ecm.1370.

Parmesan, C., Yohe, G., 2003. A globally coherent fingerprint of climate change impacts across natural systems. Nature 421 (6918), 37–42. https://doi.org/10.1038/nature01286.

Paulsen, J., Körner, C., 2014. A climate-based model to predict potential treeline position around the globe. Alpine Bot. 124, 1–12. https://doi.org/10.1007/s00035-014-0124-0.

Pepin, N., Arnone, E., Gobiet, A., Haslinger, K., Kotlarski, S., Notarnicola, C., Palazzi, E., Seibert, P., Serafin, S., Schöner, W., 2022. Climate changes and their elevational patterns in the mountains of the world. Rev. Geophys. 60 (1), e2020RG000730. https://doi.org/10.1029/2020RG000730.

Pineda, E., Lobo, J.M., 2012. The performance of range maps and species distribution models representing the geographic variation of species richness at different resolutions. Global Ecol. Biogeogr. 21 (9), 935–944. https://doi.org/10.1111/j.1466-8238.2011.00741.x.

Queirós, L., Deus, E., Silva, J., Vicente, J., Ortiz, L., Fernandes, P., Castro-Díez, P., 2020. Assessing the drivers and the recruitment potential of *Eucalyptus globulus* in the Iberian Peninsula. For. Ecol. Manag. 466, 118147. https://doi.org/10.1016/j.foreco.2020.118147.

Ray, D., Marchi, M., Rattey, A., Broome, A., 2021. A multi-data ensemble approach for predicting woodland type distribution: Oak woodland in Britain. Ecol. Evol. 11 (14), 9423–9434. https://doi.org/10.1002/ece3.7752.

Rathore, P., Roy, A., Karnatak, H., 2019. Assessing the vulnerability of Oak (*Quercus*) forest ecosystems under projected climate and land use land cover changes in Western Himalaya. Biodivers. Conserv. 28, 2275–2294. https://doi.org/10.1007/s10531-018-1679-7.

Reich, P.B., Sendall, K.M., Stefanski, A., Rich, R.L., Hobbie, S.E., Montgomery, R.A., 2018. Effects of climate warming on photosynthesis in boreal tree species depend on soil moisture. Nature 562, 263–267. https://doi.org/10.1038/s41586-018-0582-4.

Ren, Z., Peng, H., Liu, Z.-W., 2016. The rapid climate change-caused dichotomy on subtropical evergreen broad-leaved forest in Yunnan: reduction in habitat diversity and increase in species diversity. Plant Divers. 38, 142–148. https://doi.org/10.1016/j.pld.2016.04.003.

Serban, R.-D., Şerban, M., He, R., Jin, H., Li, Y., Li, X., Wang, X., Li, G., 2021. 46-year (1973–2019) permafrost landscape changes in the Hola Basin, Northeast China using machine learning and object-oriented classification. Rem. Sens. 13, 1910. https://doi.org/10.3390/rs13101910.

Shabani, F., Kumar, L., Ahmadi, M., 2016. A comparison of absolute performance of different correlative and mechanistic species distribution models in an independent area. Ecol. Evol. 6, 5973–5986. https://doi.org/10.1002/ece3.2332.

Shi, N., Naudiyal, N., Wang, J., Gaire, N.P., Wu, Y., Wei, Y., He, J., Wang, C., 2022. Assessing the impact of climate change on potential distribution of *Meconopsis punicea* and its influence on ecosystem services supply in the southeastern margin of Qinghai-Tibet Plateau. Front. Plant Sci. 12, 3338. https://doi.org/10.3389/fpls.2021.830119.

Sigdel, S.R., Wang, Y., Camarero, J.J., Zhu, H., Liang, E., Peñuelas, J., 2018. Moisture-mediated responsiveness of treeline shifts to global warming in the Himalayas. Global Change Biol. 24, 5549–5559. https://doi.org/10.1111/gcb.14428.

Sun, J., Qiu, H., Guo, J., Xu, X., Wu, D., Zhong, L., Jiang, B., Jiao, J., Yuan, W., Huang, Y., 2020. Modeling the potential distribution of *Zelkova schneideriana* under different human activity intensities and climate change patterns in China. Glob. Ecol. Conserv. 21, e00840. https://doi.org/10.1016/j.gecco.2019.e00840.

Takahashi, K., Azuma, H., Yasue, K., 2003. Effects of climate on the radial growth of tree species in the upper and lower distribution limits of an altitudinal ecotone on Mount Norikura, central Japan. Environ. Res. 18, 549–558. https://doi.org/10.1046/j.1440-1703.2003.00577.x.

Thuiller, W., Lafourcade, B., Engler, R., Araújo, M.B., 2009. BIOMOD–a platform for ensemble forecasting of species distributions. Ecography 32, 369–373. https://doi.org/10.1111/j.1600-0587.2008.05742.x.

Tiwari, A., Adhikari, A., Fan, Z.-X., Li, S.-F., Jump, A.S., Zhou, Z.-K., 2023. Himalaya to Hengduan: dynamics of alpine treelines under climate change. Reg. Environ. Change 23 (4), 157. https://doi.org/10.1007/s10113-023-02153-9.

Trujillo, E., Molotch, N.P., Goulden, M.L., Kelly, A.E., Bales, R.C., 2012. Elevation-dependent influence of snow accumulation on forest greening. Nat. Geosci. 5, 705–709. https://doi.org/10.1038/ngeo1571.

Valavi, R., Guillera-Arroita, G., Lahoz-Monfort, J.J., Elith, J., 2022. Predictive performance of presence-only species distribution models: a benchmark study with reproducible code. Ecol. Monogr. 92, e01486. https://doi.org/10.1002/ecm.1486.

Wang, A., Melton, A.E., Soltis, D.E., Soltis, P.S., 2022. Potential distributional shifts in North America of allelopathic invasive plant species under climate change models. Plant Divers 44, 11–19. https://doi.org/10.1016/j.pld.2021.06.010.

Wang, L., Wang, W.J., Wu, Z., Du, H., Zong, S., Ma, S., 2019. Potential distribution shifts of plant species under climate change in Changbai Mountains, China. Forests 10 (6), 498. https://doi.org/10.3390/f10060498.

Wang, X., Dong, W., Liu, H., Wu, Z., Fan, W., Dai, J., 2018. Population dynamics of *Betula ermanii* in response to climate change at the Changbai Mountain treeline, China. Curr. Sci. 115, 1751–1760. https://www.jstor.org/stable/26978491. (Accessed 28 April 2022).

Wielgolaski, F.E., Hofgaard, A., Holtmeier, F.-K., 2017. Sensitivity to environmental change of the treeline ecotone and its associated biodiversity in European mountains. Clim. Res. 73 (1–2), 151–166. https://doi.org/10.3354/cr01474.

Wu, M., He, H.S., Zong, S., Tan, X., Du, H., Zhao, D., Liu, K., Liang, Y., 2018. Topographic controls on vegetation changes in alpine tundra of the Changbai Mountains. Forests 9, 756. https://doi.org/10.3390/f9120756.

Xu, D., Geng, Q., Jin, C., Xu, Z., Xu, X., 2020. Tree line identification and dynamics under climate change in Wuyishan National Park based on Landsat images. Rem. Sens. 12, 2890. https://doi.org/10.3390/rs12182890.

Yu, D., Wang, G.G., Dai, L., Wang, Q., 2007. Dendroclimatic analysis of *Betula ermanii* forests at their upper limit of distribution in Changbai Mountain, Northeast China. For. Ecol. Manag. 240, 105–113. https://doi.org/10.1016/j.foreco.2006.12.014.

Yu, D., Wang, Q., Liu, J., Zhou, W., Qi, L., Wang, X., Zhou, L., Dai, L., 2014. Formation mechanisms of the alpine Erman's birch (*Betula ermanii*) treeline on Changbai Mountain in Northeast China. Trees 28, 935–947. https://doi.org/10.1007/s00468-014-1008-z.

Zhao, G., Cui, X., Sun, J., Li, T., Wang, Q., Ye, X., Fan, B., 2021. Analysis of the distribution pattern of Chinese *Ziziphus jujuba* under climate change based on optimized biomod2 and MaxEnt models. Ecol. Indicat. 132, 108256. https://doi.org/10.1016/j.ecolind.2021.108256.

Zhao, H., Zhang, H., Xu, C., 2020. Study on *Taiwania cryptomerioides* under climate change: MaxEnt modeling for predicting the potential geographical distribution. Glob. Ecol. Conserv. 24, e01313. https://doi.org/10.1016/j.gecco.2020.e01313.

Zhong, Y., Xue, Z., Davis, C.C., Moreno-Mateos, D., Jiang, M., Liu, B., Wang, G., 2022. Shrinking habitats and native species loss under climate change: a multifactorial risk assessment of China's inland wetlands. Earth's Future 10, e2021EF002630. https://doi.org/10.1029/2021EF002630.

Zong, S., Wu, Z., Xu, J., Li, M., Gao, X., He, H., Du, H., Wang, L., 2014. Current and potential tree locations in tree line ecotone of Changbai Mountains, Northeast China: the controlling effects of topography. PLoS One 9, e106114. https://doi.org/10.1371/journal.pone.0106114.